Essential oil from *Curcuma phaeocaulis* Val.: Chemical composition and anti-inflammatory activities via integrated multi-omics analysis in a zebrafish tail fin amputated model

Weiwei Sun[1†], Yao Fu[2,3†], Bo Yu[4†], Yongjia Zhang[1], Min He[2,3*], Mengmeng Sun[2,3*], Ruihua Zhao[1*]

[1]Guang'anmen Hospital, Chinese Academy of Traditional Chinese Medicine, Beijing, PR China; [2]Changchun University of Chinese Medicine, Changchun, PR China; [3]The Jilin Province School-Enterprise Cooperation Technology Innovation Laboratory of Herbal Efficacy Evaluation Based on Zebrafish Model Organisms, Changchun University of Chinese Medicine, Changchun, PR China; [4]Institute of Microelectronics, Chinese Academy of Sciences, Beijing, PR China

[†]These three authors have equal contributions

***Corresponding Authors:** Min He, Changchun University of Chinese Medicine, Changchun, PR China; and The Jilin Province School-Enterprise Cooperation Technology Innovation Laboratory of Herbal Efficacy Evaluation Based on Zebrafish Model Organisms, Changchun University of Chinese Medicine, Changchun, PR China. Email: hemin@ccucm.edu.cn; Mengmeng Sun, Changchun University of Chinese Medicine, Changchun, PR China; and The Jilin Province School-Enterprise Cooperation Technology Innovation Laboratory of Herbal Efficacy Evaluation Based on Zebrafish Model Organisms, Changchun University of Chinese Medicine, Changchun, PR China. Email: sunmm@ccucm.edu.cn; Ruihua Zhao, Guang'anmen Hospital, Chinese Academy of Traditional Chinese Medicine, Beijing, PR China. Email: rhzh801@126.com

Academic Editor: Mohammad Hashem Yousefi, PhD, Department of Food Hygiene and Public Health, School of Veterinary Medicine, Shiraz University, Shiraz, Iran

Received: 8 January 2025; Accepted: 27 June 2025; Published: 1 October 2025

RESEARCH ARTICLE

Abstract

Curcuma phaeocaulis Val. is a widely accessible herbal remedy in the Chinese medicinal materials market, yet research on the *in vivo* anti-inflammatory effects of its essential oil (ZTO) components remains somewhat limited. This study aims to evaluate the chemical composition and anti-inflammatory properties of the ZTO. The chemical composition of the ZTO was analyzed by employing gas chromatography coupled with mass spectrometry, and its anti-inflammatory properties were utilized using a zebrafish tail fin amputation model. The systematic regulatory effects on gene expression and metabolic levels were detected and analyzed using multiomics analysis, including transcriptomics and metabolomics. Thirty-five compounds were identified in ZTO, with curzerene being the main component, comprising 37.90% of the total. ZTO demonstrated significant anti-inflammatory properties by reducing neutrophil migration in zebrafish tail fin amputation models. Transcriptomics and metabolomics analyses showed that ZTO modulates inflammation through multiple pathways, aiding in the restoration of homeostasis and energy balance. These findings deepen our understanding of the anti-inflammatory mechanisms of ZTO and highlight its potential in cosmetics, food, and pharmaceuticals, emphasizing the need for further research to enhance the use of *C. phaeocaulis* Val. and related industrial products.

Keywords: *Curcuma phaeocaulis* Val.; essential oil; inflammation; metabolomics; transcriptomics; zebrafish

Introduction

Inflammation is a multifaceted immune response that arises when an organism is subjected to various inflammatory stimuli, including bacterial and viral infections, physical and chemical factors, and injuries, among others. This response is characterized by symptoms such as redness, swelling, heat generation, body aches, local dysfunction at the site of inflammation, and systemic inflammatory reactions such as fever and leukocytosis (Chopra *et al.*, 2024). Consequently, inflammation is widely considered a natural defensive mechanism that bolsters the body's resistance to pathogens (Xiang *et al.*, 2023). Nevertheless, the inflammatory response encompasses a cascade of cellular and molecular events, such as the secretion of proinflammatory mediators and the production of reactive oxygen species. When left unchecked, inflammation can disturb the equilibrium between cellular and molecular processes. Persistent cytokine circulation perpetually stimulates immune cells, potentially transforming acute inflammation into a chronic condition. This chronic state is linked to an elevated risk of developing a spectrum of diseases, including cancer, cardiovascular disease, and diabetes (Nigam *et al.*, 2023). The prolonged administration of anti-inflammatory medications, such as aspirin and ibuprofen, poses significant concerns due to their adverse effects on the normal physiological functions of healthy tissues, including the gastrointestinal tract, cardiovascular system, bone, and kidneys (Panchal and Prince Sabina, 2023). Therefore, there is a pressing need for the further discovery and development of natural, safe, and efficacious plant-based anti-inflammatory agents.

Plants have played a pivotal role in the evolution of new medications, as evidenced by Süntar in 2020 (Süntar, 2020). Essential oils extracted from various aromatic plants, characterized by their high concentration of volatile compounds, are extensively employed in the food additive and perfume and cosmetic industries, significantly advancing the industrial application and product development of essential oils. Moreover, many European and American countries have recognized the multiple potential activities, including antioxidant, anti-inflammatory, antimicrobial, analgesic, antiulcer, antidiabetic, and neuroprotective effects, possessed by various plant essential oils (Agnish *et al.*, 2022; Ammar *et al.*, 2022; De Cicco *et al.*, 2023; dos Santos *et al.*, 2021; Froz *et al.*, 2024; Huang *et al.*, 2021; Jaradat *et al.*, 2022; Li *et al.*, 2022b). Numerous nutraceuticals, food supplements, and pharmaceutical prescriptions are developed and produced leveraging the bioactivities of essential oils as their foundation. The essential oils have gained increased popularity in aromatherapies as a complementary alternative therapy in many countries, and have sparked increasing interest among researchers in the study of essential oil activities, which offer a broader spectrum of health benefits to the modern world.

Curcuma (known as "Ezhu" or "莪术" in Chinese), commonly used as food, is utilized as a traditional folk medicinal resource in some Asian countries (such as China, South Korea, and Nepal) (Figure 1A). It has a relatively ancient history in its medicinal applications, with its earliest records dating back to the Book "Compendium of Materia Medica" authored by Li Shizhen during the Ming Dynasty in China. The three different species (*Curcuma phaeocaulis* Val., *Curcuma kwangsiensis* S. G. Lee et C. F. Liang, and *Curcuma wenyujin* Y. H. Chen et C. Ling) are officially incorporated into the latest edition of Chinese Pharmacopoeia, among which the *C. phaeocaulis* Val. is one of the most widely used and distributed in the southwestern regions of China as well as in Java and Vietnam (Figure 1B). According to the Chinese Pharmacopoeia and many ancient Chinese records, the principal and traditional uses of this plant primarily include improving blood circulation and resolving blood stagnation, which in turn serves to alleviate pain and reduce swelling. Therefore, it can be employed as a complementary therapy for various conditions such as amenorrhea, menstrual pain relief, postpartum congestion, gastritis, and uterine inflammation. Additionally, it promotes healthy splenic digestion, alleviates discomfort in the chest and abdomen, strengthens spleen function, and facilitates digestion. Furthermore, it possesses antibacterial properties. These may all suggest its potential as a candidate for anti-inflammatory and analgesic drugs to mitigate traumatic injuries.

Recently, the abundance of diverse chemical constituents within this plant has been studied, including flavonoids, organic acids, and sesquiterpenes, among others. The pharmacological investigation of its alkamides reveals potential neuroprotective properties (Li *et al.*, 2022a), and that of organic acids, terpenoids, and steroids reveals antioxidant, antimelanogenesis, and antimelanogenic activities (Le *et al.*, 2025; Lee *et al.*, 2019). Additionally, the presence of monomeric and dimeric guaianolide sesquiterpenoids within this plant has been confirmed to possess hypoglycemic activity (Xue *et al.*, 2023). These therapeutic effects are closely associated with its capacity to modulate inflammatory responses and regulate the immune system functions. However, current pharmacological activity studies on *C. phaeocaulis* Val. have primarily concentrated on its water or alcohol extracts. Given that plants which belong to the Zingiberaceae family are known for their aromatic scent, essential oils are abundant in this botanical family. Nevertheless, the current research on this plant focuses on its chemical composition, including its essential oils (ZTO); limited research has focused on the anti-inflammatory potential of its essential oils.

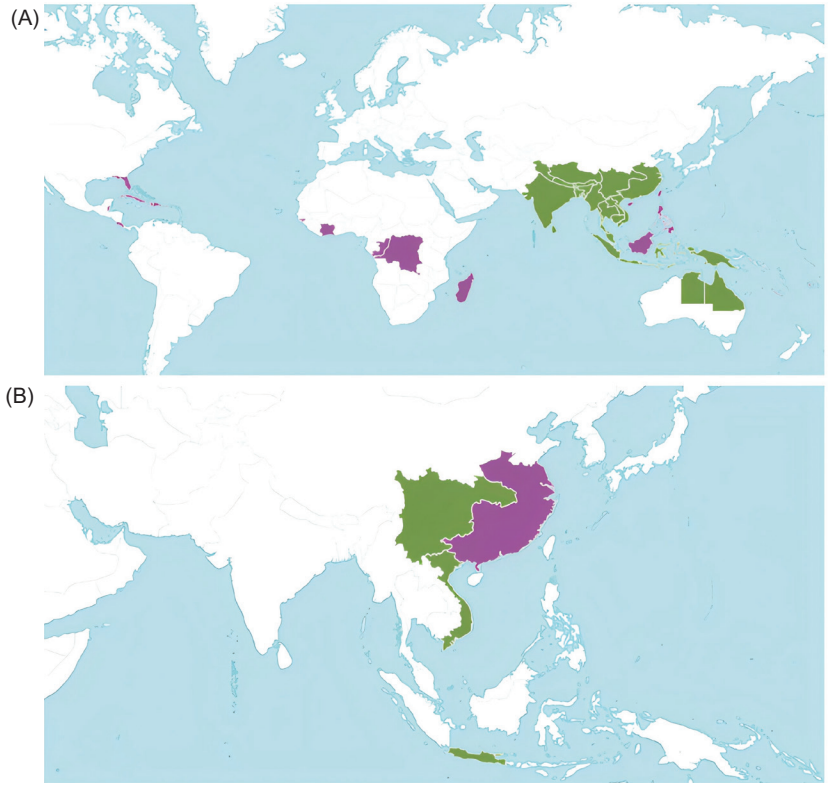

Figure 1. The geographical distribution of the *Curcuma Genus* and the special species of *Curcuma phaeocaulis* Val., based on the website of Plants of the World Online (https://powo.science.kew.org/). (A). The geographical distribution of the *Curcuma* L. and (B) the geographical distribution of the *Curcuma phaeocaulis* Val.

In this study, we examined the chemical composition of ZTO via gas chromatography-mass spectrometry (GC-MS). Subsequently, we explored the anti-inflammatory properties of ZTO employing a zebrafish tail fin amputation model. By utilizing transcriptome and metabolomic analyses, we further successfully pinpointed genes and metabolites that exhibit differential expression and significantly influence ZTO's anti-inflammatory mechanism. Additionally, pathway enrichment analysis was conducted to gain a deeper understanding of these results. Ultimately, gene expression validation was performed using RT-PCR. The findings indicate that ZTO possesses a significant anti-inflammatory effect. Consequently, our discoveries provide novel empirical evidence to elucidate the anti-inflammatory mechanism of ZTO and offer scientific support for the industrial application and utilization of *C. phaeocaulis* Val.

Materials and Methods

Chemicals

The *C. phaeocaulis* Val. was harvested from the city of Baishan (Jilin province, China). These plants underwent a rigorous and stringent verification process conducted by Professor Mengmeng Sun of the Changchun University of Chinese Medicine. The extraction of the essential oil from the *C. phaeocaulis* Val. was achieved through steam distillation, a method renowned for its effectiveness and widespread acceptance in the realm of herbal extraction. ZTO was obtained by mixing a sample of *C. phaeocaulis* Val. with water (1:10 w/v), soaking for 2 h, and then steam-distilling at 100°C for 10 h, yielding 2.40% (Zhang *et al.*, 2017).

Tween-80 was procured from Beijing Solarbio Science & Technology Co., Ltd., located in China. Additionally, other chemicals such as the positive control drug (beclomethasone), anesthetic agent (tricaine), and chemical standards were acquired from Shanghai Yuanye Bio-Technology Co., Ltd., situated in China.

The organic solvents, including ethyl acetate, trichloromethane, and isopropanol, were sourced from Sigma-Aldrich, a reputable company headquartered in St. Louis, Missouri, United States. These chemical compounds, with a purity exceeding 98% and analytical grade, serve as a guarantee for reliable and precise scientific experiments.

GC-MS analysis

A rigorous and comprehensive analysis was undertaken utilizing the sophisticated methodology of GC-MS (Cheng *et al.*, 2025). This process incorporated the 8890 gas chromatography system, which was integrated with the 7000D mass spectrometer, manufactured by Agilent Technologies in the United States. The separation phase was performed with high precision using a silica capillary column from Agilent Technologies' HP-5 ms model (30 m × 0.25 mm × 0.25 μm), ensuring efficient separation. The initial temperature of the column was set at 45°C for 2 min for conditioning, then increased to 280°C at 5°C per minute and held for 10 min to elute complex compounds. Helium was used as the carrier gas, flowing at a constant and uniform linear velocity of 2.2 mL/min, ensuring the efficient and seamless transport of the sample components through the column. The electron ionization (EI) source was operated at a temperature of 230°C, enabling the effective ionization of the compounds. The mass spectrometer was calibrated to scan across a broad range of 40–500 m/z, capturing a comprehensive spectrum of masses for detailed and exhaustive analysis. The samples were prepared by diluting them at a ratio of 10:90 (v/v) with ethyl acetate, and ensuring thorough mixing through vortex agitation, to achieve homogeneity. For the actual analysis, a precise volume of 1.0 μL of the prepared samples was accurately injected into the system. After detection, a detailed qualitative study was performed using MassHunter software. Components in the samples were determined by comparing their mass spectra with the NIST20 library. To ensure accuracy, these were cross-checked with the literature and standards. Essential oil components were quantified by measuring area percentages using peak area normalization, providing a reliable estimate of relative concentrations.

Animals

The zebrafish used in this study were obtained from the China Zebrafish Resource Center (http://www.zfish.cn/), bred and supervised according to the guidelines of the Zebrafish Model Organism Database (http://zfin.org). To maintain the natural circadian cycles of the zebrafish, a precisely controlled lighting regimen was implemented, consisting of 14 h of light exposure, followed by 10 h of darkness. Fertilization was achieved through natural spawning, which was initiated during the light phase. Subsequently, the freshly laid eggs were carefully collected and incubated in a specialized solution known as egg water, maintained at a constant temperature of 28°C. This solution was prepared to include 60 μg/mL of Instant Ocean Sea salts and supplemented with 0.0025% methylene blue to ensure an optimal environment for embryonic development (He *et al.*, 2020).

In addition to the standard wild-type zebrafish (AB strain), the study also incorporated specific transgenic lines, *Tg* (mpx:GFP), to facilitate the creation of a tail fin amputation model. This model aimed to investigate the migratory behaviors of neutrophils during the inflammatory response, particularly in response to ZTO treatment. The experimental procedures strictly adhered to the guidelines and regulations set forth by the animal welfare committee at Changchun University of Chinese Medicine. Throughout the study, all animal handling and interventions were carried out in strict accordance with the comprehensive Guidelines for the Care and Use of Laboratory Animals established by Changchun University of Chinese Medicine (No. 2024692).

Safety Test for ZTO

In the realm of scientific experimentation, 0.03% Tween-80 was employed as a cosolvent to enhance the solubility of ZTO within egg water, thereby facilitating the creation of solutions with varying concentrations of 1.0, 2.5, and 5.0 μg/mL. This approach aimed to ensure that ZTO could be effectively integrated into the aqueous medium. Subsequently, an extensive experimental evaluation was conducted to determine the safe concentration threshold of Tween-80. To this end, the 3-day-old zebrafish larvae were subjected to a controlled exposure involving solutions of egg water that contained different concentrations of ZTO in combination with Tween-80, with each experimental group consisting of 30 larvae. This exposure lasted for a continuous period of 96 h, during which the researchers conducted a thorough examination, focusing on observing and documenting any lethal effects that the ZTO/Tween-80 solutions might have on the zebrafish larvae. This observation was conducted at intervals of 24, 48, 72, and 96 h, ensuring a comprehensive understanding of the impact of the solutions over time (He *et al.*, 2020).

Zebrafish tail fin amputation tests

The experiments involving the amputation of tail fins were conducted on 3-day-old zebrafish larvae, which underwent a pretreatment phase lasting 2 h. Throughout this period, the larvae were exposed to a solution containing ZTO with 0.03% Tween-80 at varying concentrations of 0.5, 1.0, and 2.5 μg/mL, in addition to beclomethasone or egg water. In detail, each experimental group consisted of 30 larvae. After undergoing the pretreatment phase, the larvae were carefully transferred into a solution consisting of egg water supplemented with 0.02% tricaine to induce a state of anesthesia. Subsequently, these anesthetized larvae were delicately placed onto petri dishes that had been previously prepared with a coating of 2%

agarose to ensure a stable and nonadhesive surface. The precise procedure of amputation was carried out with the aid of a Leica M165C stereomicroscope, a micromanipulator for fine control, and a 1 mm sapphire blade obtained from World Precision Instruments, as detailed in the study by He *et al*. (2020). Following the amputation, the zebrafish larvae were either returned to freshly prepared ZTO solution or positive drug (beclomethasone), or kept in egg water, with a duration extending over 4 h. Each experimental group comprised three biological replicates. The use of microscopic examination on the zebrafish larvae enabled real-time monitoring, which greatly facilitated and simplified the study of neutrophil migration processes within these organisms.

Gene expression analysis

For gene expression analysis by RT-PCR, 30 zebrafish larvae from each group were treated using the same method as described above. Larval zebrafish were ground, and the total RNA was extracted with TRIZOL reagent (Thermo Fisher Scientific, USA). RNA concentration was measured by absorbance in CLARIOstar (BMG LABTECH, Germany). We used a reverse transcription kit (Tiangen Biotech Co., Ltd., China) to synthesize cDNA from 2 μg of RNA and diluted (1:10). The cDNA was amplified with SYBR Green system (Tiangen Biotech Co., Ltd., China) and CFX96 Deep Well Dx (Bio-Rad Laboratories, USA) in the RT-PCR reaction (Cheng *et al.*, 2025). The $2^{-\Delta\Delta Ct}$ method was used for quantification of gene transcription, and the transcription level of β-actin was used to normalize the relative expression of other genes in all samples. All primer sequences used for this study were from the previous literature and are presented in Table 1. Each experimental group comprised three biological replicates. RT-PCR was used to measure the levels of TNF-α, IL-1β, and IL-6 in each group.

RNA-seq assay and transcriptomic analysis

The mRNA samples underwent fragmentation with the aid of a dedicated buffer, adhering strictly to the Illumina manufacturer's protocol. Following this, a reverse transcription process was initiated, converting the fragmented mRNA into cDNA. The resulting cDNA libraries were constructed via PCR amplification of the fragmented cDNA. These libraries underwent sequencing with Illumina sequencers (HiSeq4000), utilizing paired-end technology to generate reads of 2 × 150 base pairs in length. Each experimental group comprised three biological replicates.

The raw RNA-seq data was subjected to rigorous processing using the R statistical software, specifically version 4.0.4. Before and after the quality control and adapter trimming steps, the FastQC package was employed to assess the characteristics of the reads. The Trimmomatic tool was utilized to eliminate Illumina adapters and Reads with low quality. Data were filtered by removing Reads with an average mass fraction below Q20. For normalization of gene expression levels, the TPM (Transcripts Per Million) method was applied, with genes possessing a TPM value exceeding 1 being generally considered expressed. This criterion was used to screen gene repositories and select genes for further differential expression analysis. Differential gene expression analysis was conducted utilizing DESeq, with the identification of differentially expressed genes being based on a fold change of |log2FoldChange|>0.585 and a statistically significant P-value < 0.05 (Cheng *et al.*, 2025).

Furthermore, Gene Ontology (GO, http://geneontology.org/) analysis was performed to delve into alterations in biological processes (BP), cellular components (CC), and molecular functions (MF). Additionally, Kyoto Encyclopedia of Genes and Genomes (KEGG, https://www.genome.jp/kegg/) pathway analysis was conducted using the enhanced KEGG algorithm within the clusterProfiler package.

Metabolomics analysis

The samples underwent extraction for 1 min, followed by agitation for 5 min at ambient temperature. Subsequently, they were centrifuged at 12,000 RPM for 10 min at 4°C. The resulting supernatant was then subjected to metabolomic analysis. Each group was analyzed with three biological replicates. Quality control samples were inserted during instrumental analysis to ensure data reliability.

Table 1. Sequence of primers for the RT-PCR analysis.

Gene	Forward primer sequence (5′→3′)	Reverse primer sequence (5′→3′)
β-Actin	GCCAACAGAGAGAAGATGACACAG	CAGGAAGGAAGGCTGGAAGAG
TNF-α	ACCAGGCCTTTTCTTCAGGT	TTTGCCTCCGTAGGATTCAG
IL-1β	TGGACTTCGCAGCACAAAATG	GTTCACTTCACGCTCTTGGATG
IL-6	GATGACAGTGAAGCTCTTGGACAC	CCGATTCAGTCTGACCGGAGATTG

The prepared samples were then injected into the Agilent Technologies 1290 Infinity UPLC system, equipped with an Acquity UPLC HSS T3 chromatography column (2.1 × 100 mm, 1.8 μm particle size, manufactured by Waters, Singapore) for peak separation. To achieve optimal separation speed and efficiency, the flow rate was adjusted to 0.4 mL/min. A 4 μL injection volume was utilized to ensure sufficient sample material for analysis while minimizing peak distortion due to overloading.

The mobile phase consisted of a water solution (designated as Phase A) and an acetonitrile solution (Phase B), both containing 0.1% formic acid. The gradient elution program was structured as follows: Initially, the proportion of Phase B gradually increased from 5 to 20% over 2 min to facilitate the initial elution of low polarity impurities. From 2 to 5 min, the proportion of Phase B rapidly escalated to 60% to enable the separation of medium polarity primary components. Between 5 and 6 min, the proportion of Phase B further increased to 99% to allow for the elution of high-polarity trace components. This 99% Phase B proportion was maintained until 7.5 min to ensure complete elution of all high-polarity components. From 7.5 to 7.6 min, the proportion of Phase B swiftly decreased to 5%, and this concentration was maintained for 2.4 min in preparation for the next injection.

The identification of metabolites was performed using a Mass spectrometry (Agilent 6540 UHD Accurate-Mass Q-TOF mass spectrometer), which incorporated an electrospray ionization (ESI) interface. The m/z ratio was set within the range of 50–1000, and the scan rate was maintained at 2 spectra per second. Desolation was achieved through the use of nitrogen at a temperature of 320°C, with a flow rate of 10 L/min.

Subsequently, the raw UPLC-MS data underwent conversion into the mzXML format, which was subsequently imported into the XCMS software for nonlinear alignment, time domain analysis, filtering, and extraction of peak intensities. The K-nearest neighbor algorithm was employed to fill in the blank values, and SVR regression was used to correct the peak areas. Following this process, all resulting datasets were uploaded into MetaboAnalyst 6.0 for the execution of principal component analysis (PCA). Metabolite alterations that demonstrated statistical significance between the control group and the remaining groups were identified based on a VIP score exceeding 1 and a *p*-value less than 0.05 (Cheng *et al.*, 2025). Further analyses were carried out utilizing the capabilities of MetaboAnalyst 6.0.

Statistical analysis

The experiments results were presented as the mean ± standard error of the mean (SEM) (Figures 2 and 3B–3C). Statistical analysis was performed using GraphPad Prism 9, applying a one-way ANOVA followed by Tukey's post hoc test (Figures 3B and 3C). Significance was determined at a level of $P < 0.05$, and comparisons were made between the model and control groups, each dosing group and the model group, respectively. For the analysis and visualization of omics data, we utilized the functionalities of the MetaboAnalyst 6.0 software application (PCA, heatmap), available at http://www.metaboanalyst.ca.

Results

Identification of volatile compounds in ZTO using GC-MS

Essential oils are intricate blends composed of many volatile components. Before the assessment of potential bioactivities, it is vital to thoroughly analyze the entire composition of an essential oil (Buchbauer, 2000). Based on the GC-MS, the volatile chemicals in ZTO were analyzed and identified. A total of 35 compounds were confirmed in ZTO. According to our results, the predominant component in the ZTO was curzerene, accounting for 37.90% of the total composition, followed by bicyclosesquiphellandrene and epicurzerenone, accounting for 11.29 and 7.05%, respectively. More detailed information was listed in Table 2, including the names of these compounds, molecular formula, molecular weight, their retention duration, and percentage of each chemical.

ZTO exhibits an anti-inflammatory effect, but without glucocorticoid-like side effects on inhibiting tissue regeneration in zebrafish larvae

To dissolve the oil and to evaluate the safety of ZTO, before the bioactivity test in zebrafish, we first conducted experiments with Tween-80 as a solubilizer and at various volume ratios, ranging from 0.02 to 0.06%. We confirmed that Tween-80 concentration below 0.05% was nontoxic, with the survival percentage of zebrafish larvae exceeding 80% within 96 h (Figure 2A). Consequently, to greatly minimize the potential impact of the solubilizer on the bioactivity test, we finally selected a 0.03% Tween-80 solution, which could effectively dissolve ZTO with a relative higher concentration (more than 30 μg/mL). Subsequently, the survival rates of the ZTO (dissolved 0.03% Tween-80) were evaluated using zebrafish larvae under various concentrations. The final concentration for further bioactivity tests was confirmed under the dosage ranging from 1.0 to 5.0 μg/mL, suggesting a relatively safe dosage of up to 2.5 μg/mL within 96 h (survival rate higher than 80%, Figure 2B).

Table 2. Volatile components identified in ZTO.

No.	Compound	RT (min)	Concentration (%)	Formula	MW
1	Camphene	8.78	0.49	C10H16	136.23
2	Cineole	11.26	3.11	C10H18O	154.25
3	D-Camphor	14.61	0.93	C10H18O	152.23
4	β-Elemene	21.47	0.48	C15H24	204.35
5	Bicyclogermacrene	22.55	1.30	C15H24	204.35
6	γ-Muurolene	23.10	1.24	C15H24	204.35
7	(-)-α-Gurjunene	23.63	0.75	C15H24	204.35
8	β-Selinene	23.92	1.37	C15H24	204.35
9	**Curzerene**	24.48	**37.90**	C15H20O	216.32
10	α-Bulnesene	24.62	1.32	C15H24	204.35
11	δ-Elemene	24.86	0.95	C15H24	204.35
12	β-Cadinene	25.04	0.68	C15H24	204.35
13	3,5,11-Eudesmatriene	25.43	0.53	C15H22	202.34
14	α-Costol	25.51	0.63	C15H24O	220.36
15	Selina-3,7(11)-diene	26.35	0.82	C15H24	204.35
16	Germacrone	26.62	0.53	C15H22O	218.33
17	**β-Elemenone**	26.93	**11.29**	C15H22O	218.33
18	**Epicurzerenone**	27.00	**7.05**	C15H18O2	230.30
19	γ-selinene	27.25	3.10	C15H24	204.35
20	Isospathulenol	27.46	1.73	C15H24O	220.35
21	1,2,3,4-tetra(propan-2-ylidene) cyclobutane	27.58	0.61	C15H20O	216.32
22	Guaicwood acetate	27.64	0.74	C17H28O2	264.40
23	Neointermedeol	28.04	2.00	C15H26O	222.37
24	Atractylon	28.12	1.01	C15H20O	216.32
25	γ-himachalene	28.26	0.92	C15H24	204.35
26	Neocurdione	28.34	0.78	C15H24O2	236.35
27	Squamulosone	28.89	0.99	C15H22O	218.33
28	Curdione	29.39	2.24	C15H24O2	236.35
29	6-Dehydropetasol	30.18	1.79	C15H20O2	232.32
30	4,4'-Dimethoxybiphenyl	30.61	0.48	C14H14O2	214.26
31	Isoalantolactone	30.88	0.77	C15H20O2	232.32
32	Harmalacidine	31.07	0.69	C12H12N2O2	216.24
33	Nootkaton-11,12-epoxide	31.97	3.93	C15H22O2	234.33
34	Rhizoxin	32.15	2.38	C15H22O2	234.33
35	Dehydrosanssuvea-lacton	32.66	1.66	C15H22O2	234.33
Total compounds					97.19

MW: molecular weight; RT: retention time.

According to the safety test results, we then conducted the *in vivo* anti-inflammatory studies using three different safe concentrations of ZTO (0.5, 1.0, 2.5 μg/mL) as the low, middle, and high dose treatments, respectively. A glucocorticoid, beclomethasone, at a concentration of 25 μM, was used as a positive chemical, as described in a previous study by He *et al*. (2020). Our results indicated that neutrophils exhibited a significant migration toward the site of amputation within 4 h post-operation under an inflammatory situation. The ZTO successfully inhibited the migration of neutrophils toward the amputation site (Figure 3A), based on dose dependence in zebrafish larvae, according to our statistics (Figure 3B). This effect was similar to the impact observed with beclomethasone when the dose of ZTO reached to 1.0 μg/mL.

We further utilized the same model and treatment protocols but with a longer evaluative duration, with

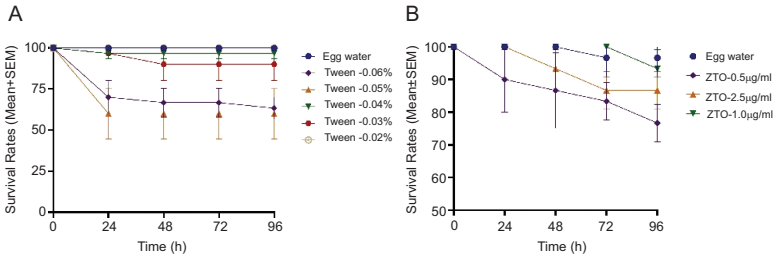

Figure 2. Experimental results of safety evaluation and anti-inflammatory activity evaluation in zebrafish model. Safety evaluation findings of Tween (A) and ZTO (B).

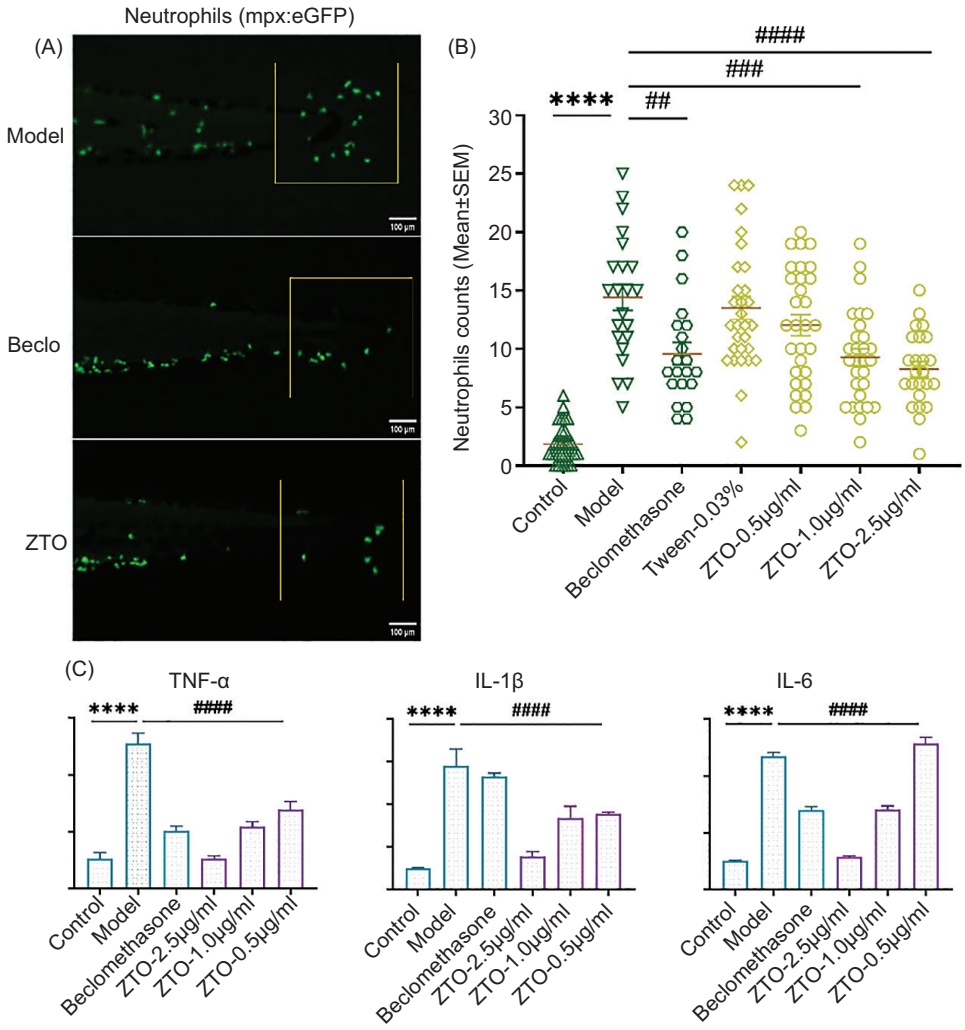

Figure 3. The anti-inflammatory effect of ZTO in a tail fin amputated zebrafish model. Neutrophils migrated toward the injury site were subjected to fluorescence imaging (A) under various treatments, including vehicle, beclomethasone, and ZTO, and subsequently underwent statistical analysis. (B) Statistical results on the number of aggregated neutrophils at the site of tail fin amputation in the zebrafish model of different groups. (C) ZTO modulates gene expression of pro-inflammatory cytokines, TNF-α, IL-1β, and IL-6. *******P* < 0.0001(in model vs control); #*P* < 0.05, ##*P* < 0.01, ###*P* < 0.001, ####*P* < 0.0001 (in treatment groups vs model).

progression at 5 dpf, to determine whether the ZTO had similar glucocorticoid-like side effects on inhibiting tissue regeneration. Upon examination, we observed that about 75% of larvae subjected to the vehicle treatment successfully regenerated their amputated tail fins, whereas larvae treated with ZTO failed to regenerate their amputated tail fins, which was consistent with our previous findings in beclomethasone (Figure 4) (He *et al.*, 2020). In summary, our findings indicate that ZTO exhibits a powerful anti-inflammatory effect following tail fin amputation, and like beclomethasone, ZTO impairs tissue regeneration even when administered at a higher concentration.

Transcriptomic analysis reveals that ZTO modulates various patterns of gene expression in zebrafish

Utilizing RNA sequencing technology, a thorough analysis of transcriptional responses was executed, culminating in the identification of 26,426 genes across the test samples. To discern these three groups at the transcriptional level, PCA was executed. Figure 5A illustrates the pronounced segregation among the three groups, with Principal Component 1 (PC1) and Principal Component 2 (PC2) accounting for 84.97 and 7.43% of the variance, respectively. Subsequently, differentially expressed genes (DEGs) were pinpointed by establishing a threshold of |log2FoldChange| exceeding 0.585 and a P-value < 0.05. As depicted in Figure 5B, we contrasted the quantity of DEGs between the model group and the control group, and between the ZTO group and the model group, respectively. In comparison with the control group, the model group modulated 68 DEGs, comprising 33 upregulated genes and 35 downregulated genes. However, upon comparing the ZTO group with the model group, the total count of DEGs amounted to 17, encompassing only 2 upregulated and 14 downregulated genes. To further clarify the quantitative correlation of DEGs between the two primary groups (model group and control group, ZTO group and model group), Figure 5C presents the corresponding Venn diagram. Five core DEGs were identified that were shared among the three groups, and Figure 5D displayed the specific expression patterns of these genes at the transcriptional level.

Then we explored the functional characteristics of these important DEGs, and $P < 0.05$ was used as the standard for GO analysis. As depicted in Figure 6A, upon utilizing the 68 DEGs that exhibited variations in the model group compared to the control group, the biological process of oxygen transport emerged as the most prominent difference. These 68 DEGs primarily pertained to the cellular component of the hemoglobin complex, as well as the molecular functions of oxygen carrier activity and oxygen binding.

In contrast, as shown in Figure 6B, the 17 DEGs that showed disparities in the ZTO-treated group compared to the model group were primarily linked to the biological process of regulating sodium ion transmembrane transporter activity. The cellular components associated with these genes encompassed nucleosomes and neuronal protection, while the molecular function revolved around cholesterol binding. In addition, the five core DEGs that were shared in the control, model, and ZTO treatments were related to the biological process of translation, the cellular component of the nucleus, and the molecular functions of RNA binding, structural constituent of ribosome, as well as molecular function (Figure 6C).

Metabolomics analysis

It is universally acknowledged that metabolism necessitates the involvement of enzymes. Irrespective of whether the constituents of enzymes are proteins or RNA, they are derivatives of gene expression within living organisms. Therefore, from this perspective, we can

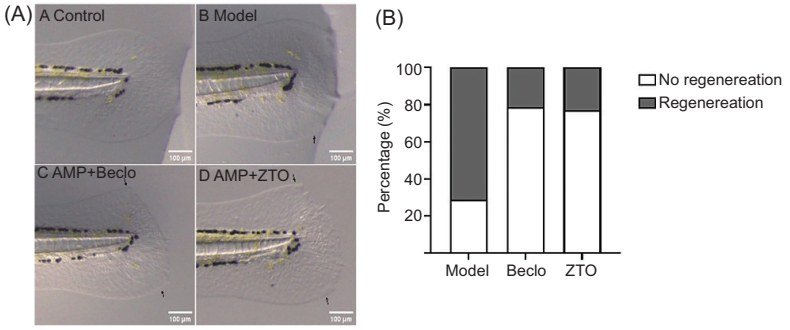

Figure 4. Effects of beclomethasone and ZTO on the regeneration of the tail fin. (A) Representative images of the tail fins of zebrafish larvae at 3 days after amputation (Amp) or without amputation (Non-Amp) and treated with vehicle, beclomethasone (Beclo), or ZTO. (B) Quantification of the tail fin regeneration in zebrafish larvae treated with Vehicle, Beclo, or ZTO (n = 30 larvae per group, with triplicates for independent experiments).

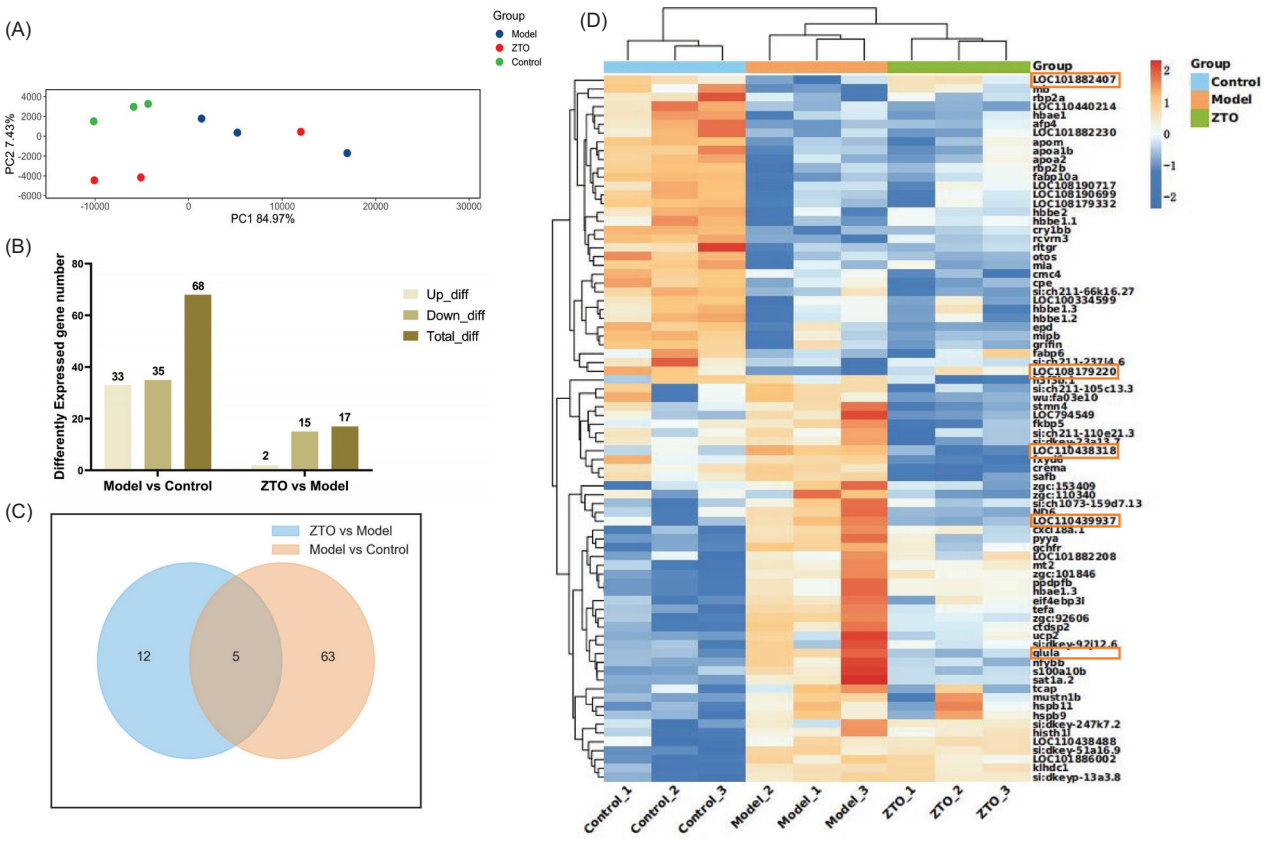

Figure 5. Expression of genes influenced by inflammatory responses and ZTO treatment: insights from transcriptomic analysis. (A) PCA score plot. (B) Statistical analysis of the number of DEGs in Model versus Control, and ZTO versus Model. (C) Venn diagram of DEGs between Model versus Control, and ZTO versus Model. (D) Heatmap of the 80 DEGs that were significantly altered by the group of Control, Model, or ZTO.

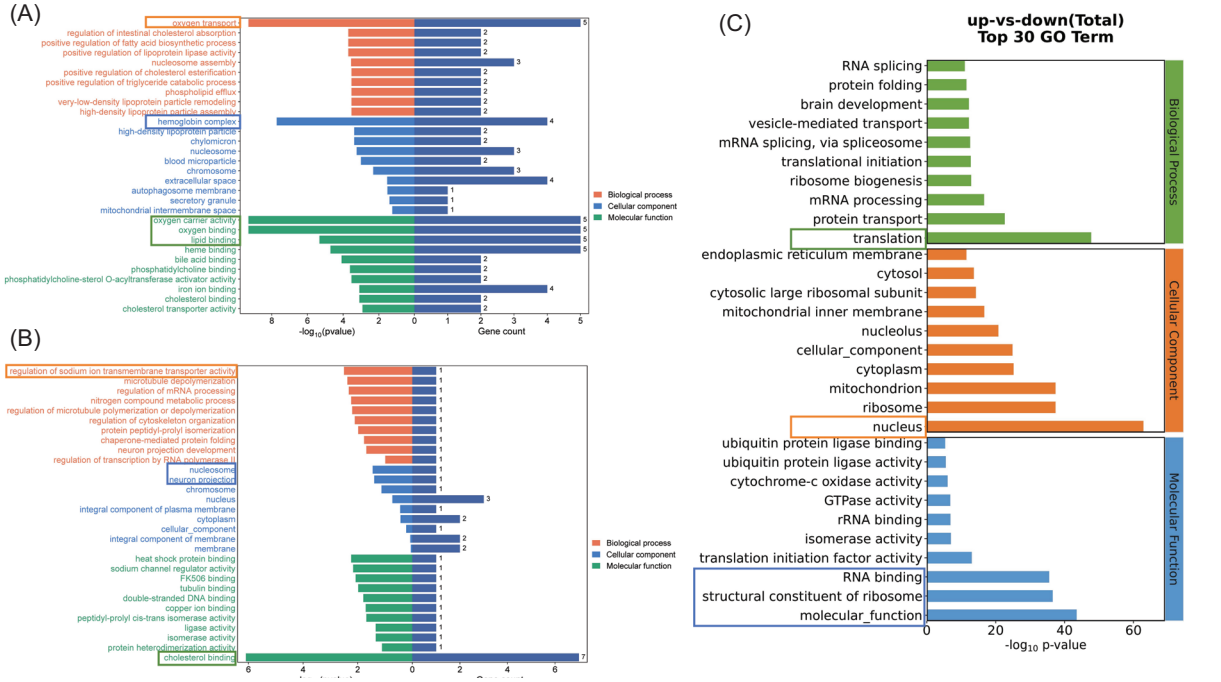

Figure 6. The GO analysis comparison using the 68 DEGs in Model versus Control (A), using the 17 DEGs in ZTO versus Model (B), and using the core DEGs shared among the 3 groups (C), respectively.

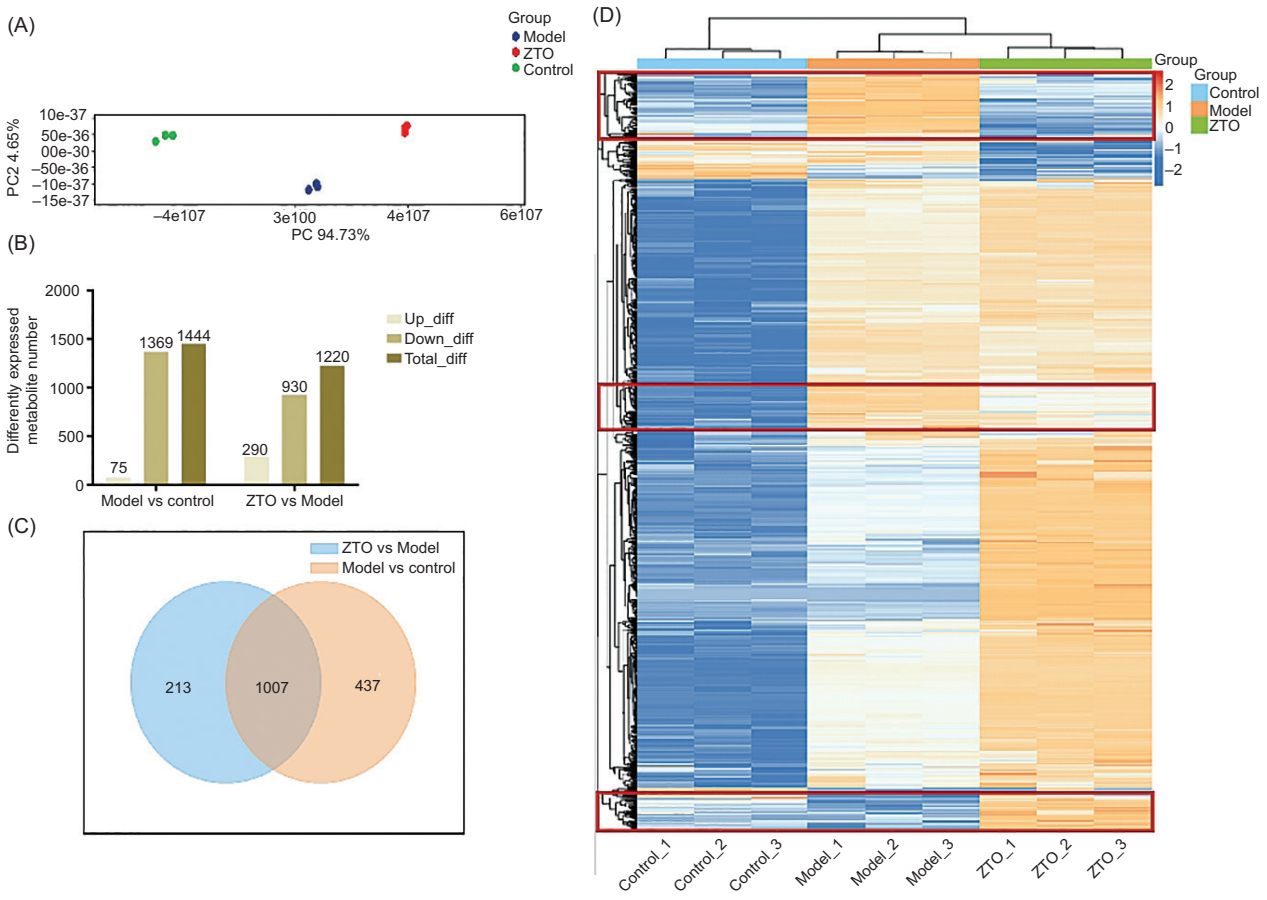

Figure 7. Metabolomics analysis results of zebrafish larvae samples with and without tail fin amputation and ZTO treatment. (A) PCA score plot. Solid circles of blue, red, and green represent the Control, Model, and ZTO groups, respectively. (B) Statistical analysis of the number of DEMs in Model versus Control and ZTO versus Model. (C) Venn diagram of DEMs between Model versus Control and ZTO versus Model. (D) Heatmap of the DEMs altered by the group of Control, Model, or ZTO.

consider that metabolites are the final products of gene expression. To further gain a deeper understanding of whether ZTO elicits changes in metabolic levels, we conducted untargeted metabolomics analyses on the control, model, and ZTO groups. The PCA results were presented as score plots in Figure 7A, clearly distinguishing the three groups. Specifically, PC1 and PC2 contribute 94.73 and 4.65%, respectively, to the overall variation. We rigorously screened and compared differentially expressed metabolites (DEMs) between groups using stringent criteria of VIP > 1.0 and $P < 0.05$. As illustrated in Figure 7B, we compared the DEMs between the model groups versus the control group, as well as the ZTO treatment versus the model groups. In comparison to the control group, the model group exhibited 1444 regulated DEMs, with 75 upregulated and 1639 downregulated genes. Similarly, in the ZTO versus model group comparison, we identified 1220 DEMs, including 290 upregulated and 930 downregulated metabolites. A Venn diagram in Figure 7C reveals all DEMs that differ between the different groups, among which 1007 are shared by the three groups. To visualize the differences in metabolic levels among the three groups for these DEMs, we generated heatmaps (Figure 7D). Many of the metabolites unequivocally indicate that the metabolic regulations by ZTO tend to call back the body status toward the healthy controls, which were marked with red box in the Figure 7D.

To further understand the metabolic pathways of these important DEMs, the metabolic pathways of these important DEMs were also analyzed via the pathway enrichment on the KEGG website (https://www.genome.jp/kegg/). In the context of the KEGG pathway enrichment analysis, our focus was specifically directed toward those metabolites that exhibited significant alterations under inflammatory conditions, yet possess the potential to restore the body's homeostasis through the intervention of ZTO, among which a total of 224 DEMs were finally screened. As depicted in Figure 8A, the pathways enriched in the inflammatory model group mainly involved energy and amino acid metabolic pathways, such as the TCA cycle, pyruvate

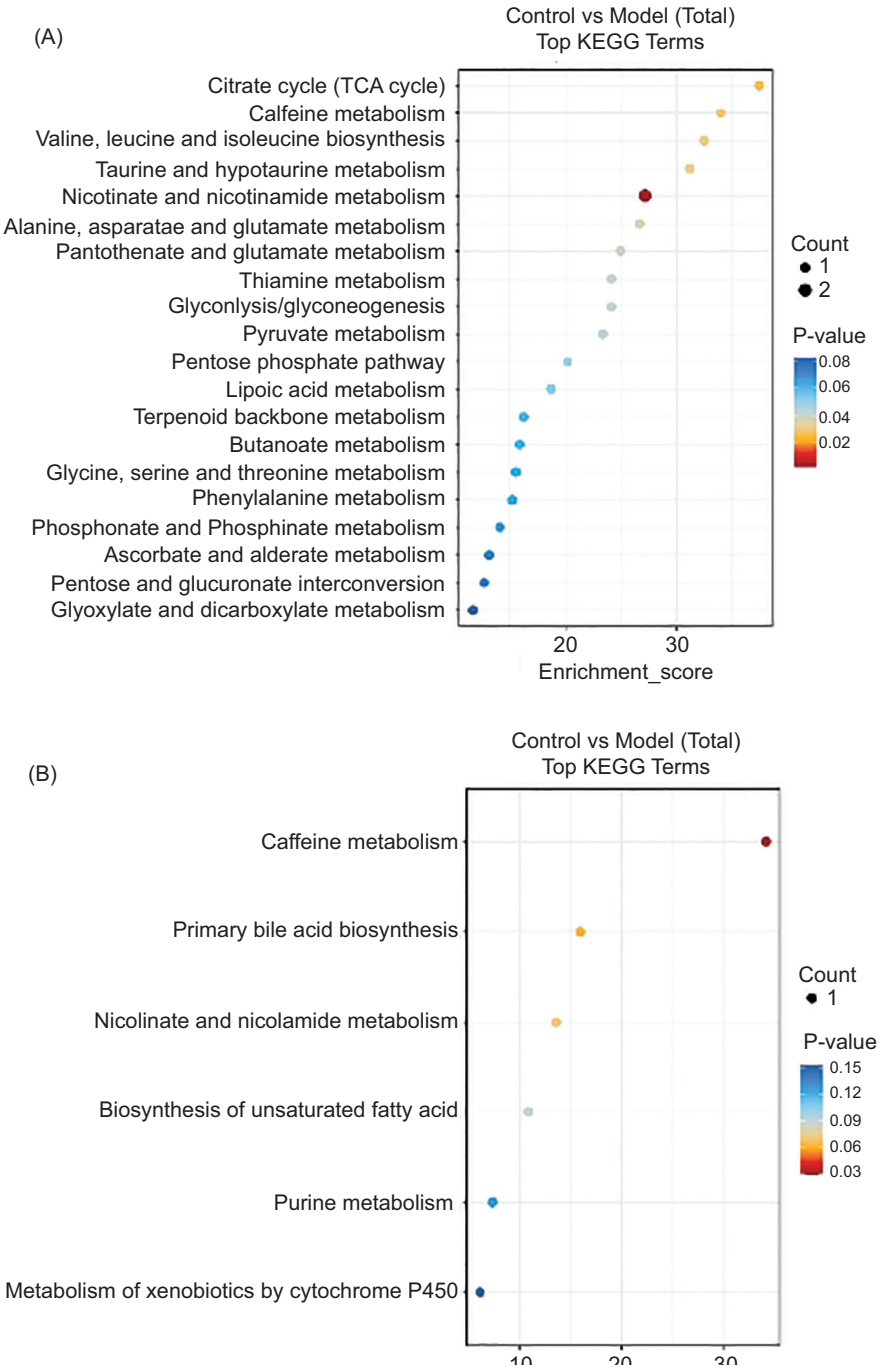

Figure 8. Metabolic pathways enrichment that were regulated by different groups. (A) The metabolic pathways in the model group versus control; and (B) that in ZTO versus Model, respectively. The pathway enrichment was examined through the analysis of 224 DEMs that showed significant changes in inflammatory states, yet can reestablish the body's equilibrium via ZTO intervention.

metabolism, valine–leucine–isoleucine biosynthesis, taurine–hypotaurine metabolism, alanine–aspartate–glutamate metabolism, glycine–serine–threonine metabolism, thiamine metabolism, lipoic acid metabolism, and phosphonate and phosphinate metabolism. Interestingly, the caffeine and nicotinate–nicotinamide metabolisms were also enriched in the inflammatory process. In contrast, the pathways enriched in the ZTO treatment group (compared to the model group) mainly involved the caffeine metabolism, Nicotinate–nicotinamide metabolism, primary bile acid biosynthesis, biosynthesis of unsaturated fatty acids, purine metabolism, and metabolism of

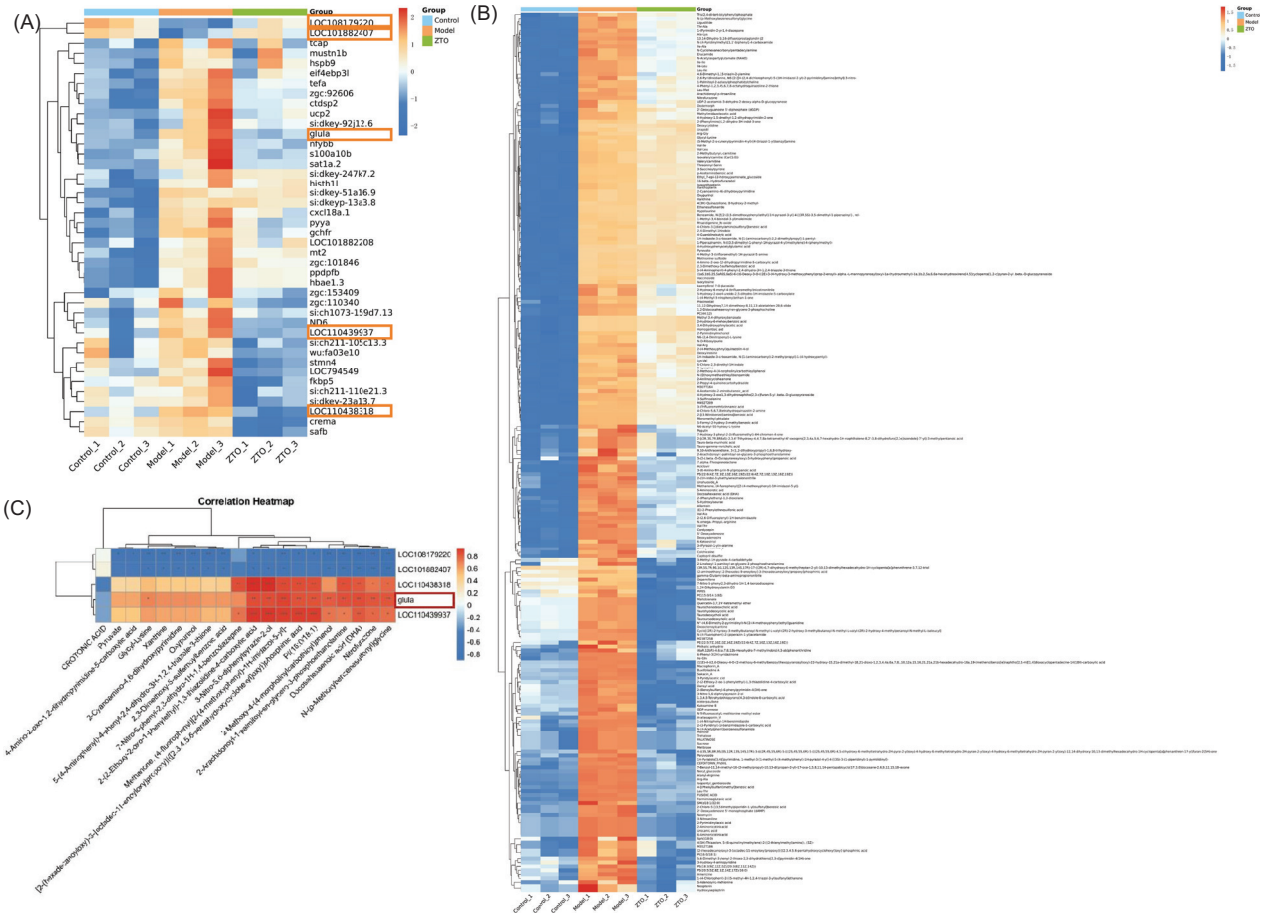

Figure 9. Heatmaps for visualizing the regulatory tendency of the important DEGs, DEMs, and the correlations among each other. (A) Heatmap of the 42 DEGs restored by the ZTO treatment against the inflammation; (B) Heatmap of the 224 DEMs restored by the ZTO treatment against the inflammation; and (C) heatmaps with strong correlations among the core DEGs and the DEMs.

xenobiotics by cytochrome P450 (Figure 8B). Notably, the core DEMs that shared in the control, model and ZTO treatment were both related to the caffeine metabolism and nicotinate and nicotinamide metabolism, which deserve further attention.

Integrated omics analysis

It is crucial for understanding the link between gene expression and metabolite levels, helping to pinpoint key metabolic pathways and regulatory genes. Therefore, we conducted an additional correlation analysis for a comprehensive and rigorous examination of the intricate interactions between transcriptomics and metabolomics data. This analysis may provide new insights for disease diagnosis and drug development, guiding the optimization of drug design and improving therapeutic outcomes by offering tools to understand complex biological networks.

For the correlation analysis, we focused on those DEGs and DEMs, which were significantly changed in the model group and could be significantly restored by the ZTO treatment. Figure 9A illustrates the 42 differentially expressed genes (DEGs), including the 5 core DEGs according to the analysis mentioned previously in Figures 5C and 5D, which can be recovered by ZTO treatment during inflammation. Additionally, Figure 9B presents the 224 significantly DEMs that were recoverable through ZTO treatment during inflammation. A correlation analysis was established and displayed in Figure 9C, based on the 5 core DEGs and the 224 important DEMs. Our correlation analysis results showed that the 5 core DEGs were strongly correlated with 20 core DEMs, among which only the *glula* gene was clearly identified. This gene was strongly correlated with 11 metabolites ($P < 0.05$). The findings may suggest that *glula*, as a pivotal gene, potentially engages in metabolic regulations, thereby modulating the inflammatory response, through which the ZTO exerts its function.

Discussion

The *C. phaeocaulis* Val. is a fascinating plant with aesthetic value, but is also often used in traditional medicine due to its various pharmacological properties, such as anti-inflammatory, antioxidant, and anticancer properties. However, there is currently limited research on the pharmacological activities of its essential oil extracts. In our study, we extract essential oil from *C. phaeocaulis* Val. to comprehensively evaluate the anti-inflammatory effect of ZTO *in vivo.* Our research concisely and explicitly elucidates that the ZTO has strong anti-inflammatory capabilities via inhibiting the neutrophil modulation, leveraging the transgenic zebrafish embryo tail fin amputation model. Furthermore, multiomics provides more technical support for our understanding of inflammatory responses and related mechanisms at the transcriptional and metabolic levels. By combining the transcriptomic and metabolomic analyses, we have discovered that the anti-inflammatory characteristics of ZTO encompass intricate genetic regulatory mechanisms that exert a substantial influence on the metabolic processes occurring within the body's various systems. The combination of transcriptomic and metabolomic analyses provides a new way to gain insight into the action of ZTO. This approach enables the simultaneous observation of changes in gene expression and metabolites at the molecular level, revealing more details about how essential oils affect metabolic pathways and biological processes in organisms.

During our analysis, through the combination analysis of multiomics, we identified 68 and 17 DEGs by comparing the model group with the control group and the ZTO group with the model group, respectively. Furthermore, five core DEGs were determined to be shared among all three groups. GO analysis indicated that during the tail fin amputation, the 68 DEGs primarily pertained to the biological process of oxygen transport emerged as the most prominent difference, and participated in the cellular component of the hemoglobin complex, as well as the molecular functions of oxygen carrier activity and oxygen binding. The transportation of oxygen throughout the body is primarily accomplished by hemoglobin within red blood cells. Oxygen binds with hemoglobin to form oxyhemoglobin, a complex that the heart circulates to tissues through the bloodstream (Riggs *et al.*, 1973). Once in the tissues, oxygen is released and enters cells to power aerobic respiration and metabolic processes. However, during inflammation, a state of hypoxia (reduced oxygen levels) may arise due to the rapid oxygen consumption by highly active immune cells and the potential disruption of microvascular function, which can exceed the oxygen supply (Williams and Chambers, 2016). Hypoxia can, in turn, exacerbate the inflammatory response by triggering the release of additional inflammatory mediators and activating signaling pathways that promote the survival and activation of immune cells, thus creating a cycle of inflammation and hypoxia (Tang *et al.*, 2023). To counter this, the body may also respond by inducing vasodilation (widening of blood vessels) in the affected area, which allows for increased blood flow to the site of inflammation and helps to deliver more oxygen-carrying red blood cells and nutrients to support the immune response, while also aiding in the removal of waste products generated during the inflammatory process. However, if self-regulation fails, medication may be required for rescue and speed up this process. Our GO enrichment results strongly confirmed that the oxygen transport process was involved in our inflammatory tail fin amputated zebrafish model.

In contrast, the 17 DEGs that were regulated by the ZTO treatment were primarily linked to the biological process of regulating sodium ion transmembrane transporter activity, and regulated the cellular components associated with these genes, encompassing nucleosomes and neuronal protection, as well as the molecular function revolved around cholesterol binding. The sodium ion transmembrane transporter activity has the potential to interact with inflammatory signaling pathways. For instance, elevation in sodium concentration may activate or inhibit specific signaling molecules integral to the inflammatory response. This can subsequently regulate genes associated with inflammation, such as those encoding cytokines, chemokines, and adhesion molecules (Grigore *et al.*, 2024; Leite *et al.*, 2020). In addition, inside cells, cholesterol modulates NF-κB activity, a key transcription factor in inflammation, influencing gene transcription of pro-inflammatory molecules. HDL, involved in reverse cholesterol transport, has anti-inflammatory effects by inhibiting immune cell activation and scavenging proinflammatory lipids (Tall and Yvan-Charvet, 2015). In summary, cholesterol binding is closely linked to inflammation, both initiating and exacerbating it, and playing a role in anti-inflammatory processes. Our results may indicate that the anti-inflammatory effect of the ZTO may be through the regulation of sodium ion transmembrane transporter activity and the cholesterol binding, which indirectly regulates the inflammatory pathways.

It is fascinating to discover that among the 5 key DEGs identified, a single core gene (*glula*) has been structurally validated. The *glula* is one of the primary sub-genotypes of the *glul* gene. The *glul* gene can encode the glutamine synthetase family, which plays a key role in amino acid metabolism, especially in the process of glutamine synthesis (Dhanasiri *et al.*, 2012; Eelen *et al.*, 2018). The ubiquitous presence of glutamate and glutamine, as key intracellular amino acids, is due to their extensive metabolic versatility. Research has shown that glutamate and glutamine can improve fish growth performance, intestinal development, and both innate and adaptive immune responses,

as well as skeletal muscle development (Li *et al.*, 2020). Furthermore, studies on mammals have identified glutamine and glutamate as functional amino acids that beneficially modulate metabolic pathways and cell signaling to enhance growth, development, and health (Wu, 2009). Under inflammatory conditions, the upregulated gene expression of the *glul* can meet the needs of immune cells for proliferation and function execution, thereby influencing the inflammatory response. The *glul* gene can help cells resist oxidative stress by promoting glutathione synthesis, protecting cells from oxidative damage. Changes in expression and activity of *glul* in various inflammation-related diseases may make it a potential target for the treatment of inflammation and related diseases. Our study has uncovered the critical role of *glula* and its associated metabolites (such as glutamate and glutamine), which are not only crucial for the early survival and development of fish, but also in alleviating inflammation.

In addition to transcriptomics, our metabolomics analysis identified DEMs between the various groups, with 1007 DEMs being shared among the three groups. Among these 1007 DEMs, a total of 224 DEMs were finally screened, which exhibited significant alterations under inflammatory conditions, yet possess the potential to restore the body's homeostasis through the intervention of ZTO. These metabolites mainly referred to the energy and amino acid metabolic pathways (e.g., TCA cycle, pyruvate metabolism, valine–leucine–isoleucine biosynthesis, taurine–hypotaurine metabolism, alanine–aspartate–glutamate metabolism, glycine–serine–threonine metabolism, thiamine metabolism, lipoic acid metabolism, and phosphonate and phosphinate metabolism). Amino acid metabolic pathways play a critical role in regulating inflammation through their involvement in immune cell function, the production of inflammatory mediators, and the overall metabolic state of the organism. For example, The TCA cycle is a central metabolic pathway that plays a crucial role in cellular energy production, as well as in the biosynthesis of various downstream biomolecules (e.g., Valine, leucine, isoleucine, taurine, hypotaurine, alanine, aspartate, glutamate, glycine, serine, and threonine) (Liu *et al.*, 2017, 2023). During an inflammatory response, immune cells undergo metabolic reprogramming to meet their increased energy demands. This is particularly evident in activated macrophages, which shift their metabolism toward increased glycolysis and changes in mitochondrial metabolism, including the TCA cycle. The TCA cycle also contributes to ATP production through oxidative phosphorylation. Activated immune cells require a significant amount of energy to support processes like proliferation, migration, and the production of inflammatory cytokines. This may explain why we find many metabolites that were associated with energy cycles were significantly upregulated under inflammatory conditions in our experiments. Understanding these interactions provides insights into how to manipulate amino acid metabolism for therapeutic benefit in inflammatory diseases.

Interestingly, the caffeine metabolism, Nicotinate–nicotinamide metabolism, primary bile acid biosynthesis, biosynthesis of unsaturated fatty acids, Purine metabolism, and metabolism of xenobiotics by cytochrome P450 were enriched in the ZTO treatment. The caffeine is a central nervous system stimulant originally found in coffee, tea, and various energy drinks. It is primarily metabolized in the liver by the cytochrome P450 enzyme system, particularly by CYP1A2. Studies have shown that caffeine exerts anti-inflammatory effects by inhibiting phosphodiesterase, which increases levels of cyclic AMP (cAMP), and by acting as an antagonist of adenosine receptors (A1 and A2A), which promotes inflammation (Cui *et al.*, 2024; Eichwald *et al.*, 2023). Nicotinate and nicotinamide are forms of vitamin B3 and are precursors for the synthesis of nicotinamide adenine dinucleotide (NAD+), which is essential for energy metabolism and redox reactions in cellular metabolism. This pathway is reported to refer to the anti-inflammation effects recently (Ma *et al.*, 2016). The biosynthesis of primary bile acids plays a crucial role not only in the digestion and absorption of fats but also in the modulation of inflammatory responses. There are some links between the primary bile acid biosynthesis and biosynthesis of unsaturated fatty acids, as well as with inflammation (Enriquez *et al.*, 2023). The bile acids are one of the main converted forms of cholesterol, which is essential for lipid metabolism and can influence fatty acid metabolism for its oxidation into oxidized lipids (oxylipins) (Guzior and Quinn, 2021; Jia *et al.*, 2021). Our metabolomics results suggest that ZTO functions systematically, not only directly downregulating inflammation through innate immune cellular regulation but also repairing the systemic damage caused by inflammation to the body. Furthermore, our integrated results, combined with correlation analysis, indicate that these systematic changes in genetic expression and metabolic pathways are closely linked, which, to some extent, corroborates our hypothesis.

Conclusions

In conclusion, our comprehensive study conclusively establishes that ZTO exerts a regulatory influence on the inflammatory response by inhibiting the aggregation of neutrophils in the zebrafish tail fin model. Through a rigorous integration of transcriptomic data, we have unveiled pivotal processes, such as oxygen transportation, sodium ion transmembrane transporter activity, nucleosomes, and neuronal protection, as well as molecular functions centered around cholesterol binding. Our metabolomic analyses revealed that ZTO even

systematically regulated the metabolism of the inflamed body, including amino acid metabolic pathways, caffeine metabolism, nicotinate–nicotinamide metabolism, primary bile acid biosynthesis, biosynthesis of unsaturated fatty acids, purine metabolism, and metabolism of xenobiotics by cytochrome P450, all of which contribute to the alleviation of inflammation. Many of the metabolites referred to these metabolic pathways showed strong correlations with the core gene of the *glula*, indicating its importance for not only early nutritional support but also inflammatory rescue for restoring the body's homeostasis and energy balance. Our findings offer a comprehensive understanding of the fundamental mechanisms that underpin ZTO's regulatory function in inflammation. As a result, this research provides invaluable scientific insights that not only enhance the optimal utilization of *C. phaeocaulis* Val. resources but also significantly contribute to the advancement of related industrial product development.

Data Availability Statement

The datasets used in this study are available from the corresponding author upon reasonable request.

Acknowledgments

The authors thank Zhongfeng Chen and Guanshu Biotechnology Services (Changchun) Co., Ltd. for providing the technical guidance.

Authors' Contributions

Weiwei Sun: Conceptualization, Methodology, Visualization, Writing - review & editing. Yao Fu: Writing – original draft, Methodology, Investigation, Data curation, Formal analysis, Visualization, Validation. Bo Yu: Formal analysis, Visualization, Validation. Yongjia Zhang: Investigation, Data curation, Formal analysis. Min He: Conceptualization, Writing – original draft, Writing – review & editing, Supervision, Funding acquisition. Mengmeng Sun: Conceptualization, Writing – review & editing, Supervision, Funding acquisition. Ruihua Zhao: Conceptualization, Writing – review & editing, Funding acquisition.

Conflicts of Interest

The authors declare that they have no known competing financial interests or personal relationships that could have appeared to influence the work reported in this article.

Funding

This research is financially supported by the National Natural Science Foundation of China (No. 82074485); the National Natural Science Foundation of China (No. 82374513); the Open Scientific Project of Institute of Basic Theory for Chinese Medicine, China Academy of Chinese Medical Sciences (No. YZX-202207); the Jilin Provincial Development and Reform Commission (No. 2023C028-1); the Pilotscale Selection Project of Colleges and Universities in Changchun City (No. 24GXYSZZ10); the Ministry of Human Resources and Social Security of the People's Republic of China high-level talent project (No. 030102070; No. 030102071).

References

Agnish, S., Sharma, A.D. and Kaur, I., 2022. Nanoemulsions (O/W) containing Cymbopogon pendulus essential oil: Development, characterization, stability study, and evaluation of in vitro anti-bacterial, anti-inflammatory, anti-diabetic activities. BioNanoScience 12(2): 540–554. https://doi.org/10.1007/s12668-022-00964-4

Ammar, N.M., Hassan, H.A., Ahmed, R.F., El-Gendy, A.E.G., Abd-ElGawad, A.M., Farrag, A.R.H., et al. 2022. Gastro-protective effect of Artemisia Sieberi essential oil against ethanol-induced ulcer in rats as revealed via biochemical, histopathological and metabolomics analysis. Biomarkers 27(3): 247–257. https://doi.org/10.1080/1354750X.2021.2025428

Buchbauer, G., 2000. The detailed analysis of essential oils leads to the understanding of their properties. Chemical Weekly-Bombay 45(49): 163–165.

Cheng, J., Fu, Y., Meng, X., Tang, G., Li, L., Yusupov, Z., et al. 2025. Investigation of anti-inflammatory effect of essential oil extracted from *Achillea alpina* L. through multi-omics analysis in zebrafish tail fin amputation model. Journal of Ethnopharmacology 344: 119519. https://doi.org/10.1016/j.jep.2025.119519

Chopra, D., Shukla, S., Rana, P., Kamar, M.D., Gaur, P., Bala, M., et al. 2024. Overview of Inflammation. In: Tripathi, A., Dwivedi, A., Gupta, S. and Poojan, S., editors. Inflammation resolution and chronic diseases. Singapore: Springer Nature. pp. 1–18. https://doi.org/10.1007/978-981-97-0157-5_1

Cui, X., Wei, W., Zhang, Z., Liu, K., Zhao, T., Zhang, J., et al. 2024. Caffeine impaired acupuncture analgesia in inflammatory pain by blocking adenosine A1 receptor. The Journal of Pain 25(4): 1024–1038. https://doi.org/10.1016/j.jpain.2023.10.025

De Cicco, P., Ercolano, G., Sirignano, C., Rubino, V., Rigano, D., Ianaro, A., et al. 2023. Chamomile essential oils exert anti-inflammatory effects involving human and murine macrophages: Evidence to support a therapeutic action. Journal of Ethnopharmacology 311: 116391. https://doi.org/10.1016/j.jep.2023.116391

Dhanasiri, A.K.S., Fernandes, J.M.O. and Kiron, V., 2012. Glutamine synthetase activity and the expression of three glul paralogues

in zebrafish during transport. Comparative Biochemistry and Physiology Part B: Biochemistry and Molecular Biology 163(3): 274–284. https://doi.org/10.1016/j.cbpb.2012.06.003

dos Santos, E., Leitão, M.M., Aguero Ito, C.N., Silva-Filho, S.E., Arena, A.C., Silva-Comar, F.M.d.S., et al. 2021. Analgesic and anti-inflammatory articular effects of essential oil and camphor isolated from *Ocimum kilimandscharicum* Gürke leaves. Journal of Ethnopharmacology 269: 113697. https://doi.org/10.1016/j.jep.2020.113697

Eelen, G., Dubois, C., Cantelmo, A.R., Goveia, J., Brüning, U., DeRan, M., et al. 2018. Role of glutamine synthetase in angiogenesis beyond glutamine synthesis. Nature 561(7721): 63–69. https://doi.org/10.1038/s41586-018-0466-7

Eichwald, T., Solano, A.F., Souza, J., de Miranda, T.B., Carvalho, L.B., dos Santos Sanna, P.L., et al. 2023. Anti-inflammatory effect of caffeine on muscle under lipopolysaccharide-induced inflammation. Antioxidants 12(3): 554. https://doi.org/0.3390/antiox12030554

Enriquez, A.B., ten Caten, F., Ghneim, K., Sekaly, R.-P. and Sharma, A.A., 2023. Regulation of immune homeostasis, inflammation, and HIV persistence by the microbiome, short-chain fatty acids, and bile acids. Annual Review of Virology 10(10): 397–422. https://doi.org/10.1146/annurev-virology-040323-082822

Froz, M.J.d.L., Barros, L.d.S.P., de Jesus, E.N.S., Tavares, M.S., Mourão, R.H.V., Silva, R.C., et al. 2024. Lippia alba essential oil: A powerful and valuable antinociceptive and anti-inflammatory medicinal plant from Brazil. Journal of Ethnopharmacology 333: 118459. https://doi.org/10.1016/j.jep.2024.118459

Grigore, A., Vatasescu-Balcan, A., Stoleru, S., Zugravu, A., Poenaru, E., Engi, M., et al. 2024. Experimental research on the influence of ion channels on the healing of skin wounds in rats. Processes 12(1): 109. https://doi.org/10.3390/pr12010109

Guzior, D.V. and Quinn, R.A., 2021. Review: Microbial transformations of human bile acids. Microbiome 9(1): 140. https://doi.org/10.1186/s40168-021-01101-1

He, M., Halima, M., Xie, Y., Schaaf, M.J.M., Meijer, A.H. and Wang, M., 2020. Ginsenoside Rg1 acts as a selective glucocorticoid receptor agonist with anti-inflammatory action without affecting tissue regeneration in zebrafish larvae. Cells 9(5): 1107. https://doi.org/10.3390/cells9051107

Huang, K., Liu, R., Zhang, Y. and Guan, X., 2021. Characteristics of two cedarwood essential oil emulsions and their antioxidant and antibacterial activities. Food Chemistry 346: 128970. https://doi.org/10.1016/j.foodchem.2020.128970

Jaradat, N., Qneibi, M., Hawash, M., Al-Maharik, N., Qadi, M., Abualhasan, M.N., et al. 2022. Assessing *Artemisia arborescens* essential oil compositions, antimicrobial, cytotoxic, anti-inflammatory, and neuroprotective effects gathered from two geographic locations in Palestine. Industrial Crops and Products 176: 114360. https://doi.org/10.1016/j.indcrop.2021.114360

Jia, W., Wei, M., Rajani, C. and Zheng, X., 2021. Targeting the alternative bile acid synthetic pathway for metabolic diseases. Protein & Cell 12(5): 411–425. https://doi.org/10.1007/s13238-020-00804-9

Le, T.T., Ha, M.T., Lee, G.S., Nguyen, V.P., Kim, C.S., Kim, J.A., et al. 2025. Terpenoids and steroids from aerial parts of *Achillea alpina* L. as PTP1B inhibitors: Kinetic analysis and molecular docking studies. Phytochemistry 229: 114269. https://doi.org/10.1016/j.phytochem.2024.114269

Lee, H.J., Sim, M.O., Woo, K.W., Jeong, D.-E., Jung, H.K., An, B., et al. 2019. Antioxidant and antimelanogenic activities of compounds isolated from the aerial parts of *Achillea alpina* L. Chemistry & Biodiversity 16(7): e1900033. https://doi.org/10.1002/cbdv.201900033

Leite, J.A., Isaksen, T.J., Heuck, A., Scavone, C. and Lykke-Hartmann, K., 2020. The α2 Na+/K+-ATPase isoform mediates LPS-induced neuroinflammation. Scientific Reports 10(1): 14180. https://doi.org/10.1038/s41598-020-71027-5

Li, X.-W., Yue, H.-C., Wu, X., Guo, Q., Tian, J.-Y., Liu, Z.-Y., et al. 2022. Neuroprotective alkamides from the aerial parts of *Achillea alpina* L. Chemistry & Biodiversity 19(7): e202200218. https://doi.org/10.1002/cbdv.202200218

Li, X., Zheng, S. and Wu, G., 2020. Nutrition and metabolism of glutamate and glutamine in fish. Amino Acids 52(5): 671–691. https://doi.org/10.1007/s00726-020-02851-2

Li, Y.-x., Erhunmwunsee, F., Liu, M., Yang, K., Zheng, W. and Tian, J., 2022. Antimicrobial mechanisms of spice essential oils and application in food industry. Food Chemistry 382: 132312. https://doi.org/10.1016/j.foodchem.2022.132312

Liu, P.-S., Wang, H., Li, X., Chao, T., Teav, T., Christen, S., et al. 2017. α-ketoglutarate orchestrates macrophage activation through metabolic and epigenetic reprogramming. Nature Immunology 18(9): 985–994. https://doi.org/10.1038/ni.3796

Liu, R., Gao, Y., Huang, L., Shi, B., Yin, X. and Zou, S., 2023. Alpha-ketoglutarate up-regulates autophagic activity in peri-implant environment and enhances dental implant osseointegration in osteoporotic mice. Journal of Clinical Periodontology 50(5): 671–683. https://doi.org/10.1111/jcpe.13784

Ma, Y., Bao, Y., Wang, S., Li, T., Chang, X., Yang, G., et al. 2016. Anti-inflammation effects and potential mechanism of Saikosaponins by regulating nicotinate and nicotinamide metabolism and arachidonic acid metabolism. Inflammation 39(4): 1453–1461. https://doi.org/10.1007/s10753-016-0377-4

Nigam, M., Mishra, A.P., Deb, V.K., Dimri, D.B., Tiwari, V., Bungau, S.G., et al. 2023. Evaluation of the association of chronic inflammation and cancer: Insights and implications. Biomedicine & Pharmacotherapy 164: 115015. https://doi.org/10.1016/j.biopha.2023.115015

Panchal, N.K. and Prince Sabina, E., 2023. Non-steroidal anti-inflammatory drugs (NSAIDs): A current insight into its molecular mechanism eliciting organ toxicities. Food and Chemical Toxicology 172: 113598. https://doi.org/10.1016/j.fct.2022.113598

Riggs, T.E., Shafer, A.W. and Guenter, C.A., 1973. Acute changes in oxyhemoglobin affinity effects on oxygen transport and utilization. The Journal of Clinical Investigation 52(10): 2660–2663. https://doi.org/10.1172/JCI107459

Süntar, I., 2020. Importance of ethnopharmacological studies in drug discovery: Role of medicinal plants. Phytochemistry Reviews 19(5): 1199–1209. https://doi.org/10.1007/s11101-019-09629-9

Tall, A.R. and Yvan-Charvet, L., 2015. Cholesterol, inflammation and innate immunity. Nature Reviews Immunology 15(2): 104–116. https://doi.org/10.1038/nri3793

Tang, Y.-Y., Wang, D.-C., Wang, Y.-Q., Huang, A.-F. and Xu, W.-D., 2023. Emerging role of hypoxia-inducible factor-1α in inflammatory autoimmune diseases: A comprehensive review. Frontiers in Immunology 13: 1073971. https://doi.org/10.3389/fimmu.2022.1073971

Williams, A.E. and Chambers, R.C., 2016. Neutrophils and tissue damage: Is hypoxia the key to excessive degranulation? Thorax 71(11): 977. https://doi.org/10.1136/thoraxjnl-2016-208879

Wu, G., 2009. Amino acids: Metabolism, functions, and nutrition. Amino Acids 37(1): 1–17. https://doi.org/10.1007/s00726-009-0269-0

Xiang, Y., Zhang, M., Jiang, D., Su, Q. and Shi, J., 2023. The role of inflammation in autoimmune disease: a therapeutic target. Frontiers in Immunology 14. https://doi.org/10.3389/fimmu.2023.1267091

Xue, G.-M., Zhao, C.-G., Xue, J.-F., Duan, J.-J., Pan, H., Jia, Y.-Y., et al. 2023. Monomeric and dimeric guaianolide sesquiterpenoids with hypoglycemic activity from *Achillea alpina*. Fitoterapia 166: 105472. https://doi.org/10.1016/j.fitote.2023.105472

Zhang, L., Yang, Z., Wei, J., Su, P., Pan, W., Zheng, X., et al. 2017. Essential oil composition and bioactivity variation in wild-growing populations of *Curcuma phaeocaulis* Valeton collected from China. Industrial Crops and Products 103: 274–282. https://doi.org/10.1016/j.indcrop.2017.04.019